Journal of Hydrology 509 (2014) 245–256

Contents lists available at ScienceDirect

Journal of Hydrology

journal homepage: www.elsevier.com/locate/jhydrol

Water table fluctuations and soil biogeochemistry: An experimental approach using an automated soil column system

F. Rezanezhad [a,*], R.-M. Couture [a,b], R. Kovac [a], D. O'Connell [a], P. Van Cappellen [a]

[a] Ecohydrology Research Group, University of Waterloo, Canada
[b] Norwegian Institute for Water Research-NIVA, Norway

ARTICLE INFO

Article history:
Received 16 May 2013
Received in revised form 19 November 2013
Accepted 22 November 2013
Available online 1 December 2013
This manuscript was handled by Peter K. Kitanidis, Editor-in-Chief, with the assistance of Martin Thullner, Associate Editor

Keywords:
Water table fluctuations
Redox conditions
Soil geochemistry
Soil respiration
Microbial communities

SUMMARY

Water table fluctuations significantly affect the biological and geochemical functioning of soils. Here, we introduce an automated soil column system in which the water table regime is imposed using a computer-controlled, multi-channel pump connected to a hydrostatic equilibrium reservoir and a water storage reservoir. The potential of this new system is illustrated by comparing results from two columns filled with 45 cm of the same homogenized riparian soil. In one soil column the water table remained constant at −20 cm below the soil surface, while in the other the water table oscillated between the soil surface and the bottom of the column, at a rate of 4.8 cm d^{-1}. The experiment ran for 75 days at room temperature (25 ± 2 °C). Micro-sensors installed at −10 and −30 cm below the soil surface in the stable water table column recorded constant redox potentials on the order of 600 and −200 mV, respectively. In the fluctuating water table column, redox potentials at the same depths oscillated between oxidizing (~700 mV) and reducing (~−100 mV) conditions. Pore waters collected periodically and solid-phase analyses on core material obtained at the end of the experiment highlighted striking geochemical differences between the two columns, especially in the time series and depth distributions of Fe, Mn, K, P and S. Soil CO_2 emissions derived from headspace gas analysis exhibited periodic variations in the fluctuating water table column, with peak values during water table drawdown. Transient redox conditions caused by the water table fluctuations enhanced microbial oxidation of soil organic matter, resulting in a pronounced depletion of particulate organic carbon in the midsection of the fluctuating water table column. Denaturing Gradient Gel Electrophoresis (DGGE) revealed the onset of differentiation of the bacterial communities in the upper (oxidizing) and lower (reducing) soil sections, although no systematic differences in microbial community structure between the stable and fluctuating water table columns were detected.

1. Introduction

The transition zone separating the soil from the underlying groundwater plays a major role in regulating the flows of carbon, nutrients and contaminants at the watershed scale (Hancock et al., 2005; Hefting et al., 2004; Sophocleous, 2002; Triska et al., 1989). The capillary fringe and the adjacent unsaturated and saturated zones are characterized by steep physical–chemical gradients, which tend to focus biogeochemical activity. Of particular importance are the concentration gradients of electron donors and acceptors, as they are intimately linked to the pathways, rates and products of many biogeochemical processes (Borch et al., 2010). In addition to spatial gradients, fluctuations in the water table may cause large temporal variations in local redox conditions (Vorenhout et al., 2004; Haberer et al., 2012), soil water content and matric potential. The limited existing data indicate that oscillating redox conditions modify the biogeochemical and microbial dynamics of subsurface environments (Blodau and Moore, 2003; Pett-Ridge et al., 2006; Weber et al., 2009), while changes in soil matric potential may further affect the mobility of organic substrates and the diffusion of nutrients and gases (Drenovsky et al., 2004; Griffiths et al., 2005; Schimel et al., 2007).

Variations in the position of the water table and the associated variations in redox conditions may impart unique geochemical and mineralogical signatures to the soil interval over which the water table fluctuates. One example is the presence in this interval of mixed valence iron minerals of the green rust group (Trolard et al., 2007). Microbial communities in the same depth interval may adapt to the continuous changes in water saturation and redox potential by developing a greater functional diversity and flexibility, compared to subsurface communities living under more

* Corresponding author. Address: Ecohydrology Research Group, Department of Earth and Environmental Sciences, University of Waterloo, 200 University Avenue West, Waterloo, Ontario N2L 3G1, Canada. Tel.: +1 (519) 888 4567x31328; fax: +1 (519) 746 7484.
E-mail address: frezanez@uwaterloo.ca (F. Rezanezhad).

0022-1694/$ - see front matter © 2013 Elsevier B.V. All rights reserved.
http://dx.doi.org/10.1016/j.jhydrol.2013.11.036

stable conditions (Pett-Ridge and Firestone, 2005). Redox oscillations have been proposed to result in a more complete degradation of organic matter in bioturbated marine sediments (Aller, 1994), but a similar effect of redox oscillations on soil organic matter degradation remains to be unequivocally demonstrated (Pulleman and Tietema, 1999). As soil microbial activity is intimately linked to the dynamics of biogenic gases (CO_2, CH_4, N_2O, methylated products), water table fluctuations are also expected to modulate gas exchanges with the atmosphere (Bubier et al., 1995; Moore and Knowles, 1989; Yavitt et al., 1997; Haberer et al., 2012).

One approach to unravel the biogeochemical implications of water table fluctuations is to conduct experiments with soil columns in which the position of the water table can be manipulated. Previous column studies have typically relied on a manual adjustment of the water table (Dobson et al., 2007; Legout et al., 2009; Farnsworth et al., 2012; Sinke et al., 1998; Williams and Oostrom, 2000). Here, we introduce a novel soil column system where the time course of the water level is imposed via a programmable multichannel pump. The system allows one to run two soil columns in parallel, with independent, pre-determined adjustment of the water levels. The use of the system is illustrated by presenting the results of an experiment with two columns that initially contained the same homogenized riparian soil. In one column the water table was maintained at a constant, mid-column level, while in the other the water level continuously oscillated. For the latter, the amplitude and periodicity of the water table fluctuations were representative of those observed in the watershed where the soil was collected. The average water depth in the fluctuating water table column coincided with the constant water level in the stable water table column.

The goal of the experiment was to better delineate the role of water table oscillations in the biogeochemical functioning of soils, by comparing soil respiration and geochemical properties under the stable and fluctuating water table regimes. Our hypothesis was that the most pronounced differences in organic carbon mineralization rates, microbial community structure and soil geochemistry would be found in the midsection of the columns, that is, within the depth interval where redox conditions and water content would deviate most significantly between the two soil columns. In addition to monitoring CO_2 emissions from the columns, pore waters were sampled periodically to follow the time-dependent distributions of diagnostic aqueous constituents. Vertical solid-phase concentrations of selected cations (Ca, K, Na), redox-active metals (Fe, Mn), organic carbon and nutrient elements (P, N, Si, S) were measured at the end of the 75-day experiment, in order to evaluate the effects of water table oscillations on soil biogeochemical transformations, elemental redistributions and the resulting geochemical depth profiles. To assess whether distinctive phylogenetic signatures emerged under the two different water table regimes, we extracted and compared DNA from the soil columns at the beginning and end of the experiment.

2. Materials and methods

2.1. Soil column system

A schematic diagram of the column set-up is shown in Fig. 1 (A picture of the experimental setup is provided as Supplementary Fig. 1). The columns, including the soil column and two auxiliary (equilibrium and storage) columns, are made of hard acrylic (wall thickness: 0.6 cm, inner diameter: 7.5 cm, length: 60 cm, Soil Measurement Systems, LLC, USA, model CL-021). The auxiliary columns control the water table level. The soil column has regularly spaced ports for sensors and pore water sampling. A filter membrane (Soil Measurement Systems, LLC, USA, bubbling pressure: 600 mbar) closes off the bottom of the column and a nylon mesh (Soil Measurement Systems, LLC, USA, bubbling pressure: 32 mbar) the top. For each column, three steel rods connect the acrylic top and bottom lids and are secured with bolts. Each lid has two ports. The entire system consists of two identical sets of three columns, which can be run in parallel.

As the labels imply, the equilibrium column is used to set the position of the water level in the soil column, while the storage column supplies water during water table rise and stores it during drawdown. A computer-controlled, multi-channel pump (9-channel Tower II pump, CAT. M. Zipperer, GmbH, Germany) regulates the flow of water between the columns. Each channel of the pump can be operated independently, with flow rates ranging from 5 μl min^{-1} to 10 ml min^{-1}. The three columns are connected to one another with chemically resistant blue polyurethane tubing (*Ark-Plas Products Inc*, *USA*, Cole-Parmer #95867-22) as illustrated in Fig. 1. When pump channel A or B is activated, the water level in the soil and equilibrium columns is lowered or raised, respectively.

The column system can be operated in a variety of configurations and water level regimes. In the configuration used here, the soil surface was kept exposed to air by having one of the ports of the upper lid open at all times (Fig. 1). To minimize evaporative water loss, the port has only a small opening (3 mm diameter). Except for this port, the system was kept completely airtight. The headspaces of the soil column and the two auxiliary columns were connected. That is, no attempt was made to exclude oxygen from the water in the auxiliary columns. For other applications, it is possible to use the upper ports of the columns to flush the headspaces with a given gas or gas mixture, for example when strict anoxic conditions need to be maintained.

2.2. Soil

The two soil columns contained soil from the riparian zone of Laurel Creek near the campus of the University of Waterloo (43°28′13″N, 80°33′20″W). The upper 15 cm of soil was collected along the unvegetated bank of the creek on October 20, 2011. By selecting an unvegetated soil, effects related to plant activity, including root respiration and exudation, were eliminated from the experiment. Surface water from the creek was obtained at the same location. The sediment was manually homogenized before introducing it into the columns. Both soil columns were packed with 45 cm of soil, leaving a headspace of 650 cm^3. In what follows, all depths are referenced with respect to the soil surface.

Basic physical and hydraulic properties of the homogenized and repacked soil, including porosity, bulk density and hydraulic conductivity, were measured using standard procedures (Klute and Dirksen, 1986). The bulk density (ρ_b) was determined gravimetrically after oven-drying the soil at 105 °C for 24 h (Gardner, 1986). The saturated hydraulic conductivity (K_{sat}) was determined using the constant head method. Soil moisture content was determined gravimetrically after drying approximately 20 g of fresh soil at 105 °C for at least 48 h. Values of K_{sat}, porosity and ρ_b were 310 cm day^{-1}, 0.43 and 1.04 g cm^{-3}, respectively.

Powder X-ray diffraction (XRD) on freeze-dried samples of the homogenized soil revealed the presence of quartz, feldspars, Ca and Mg carbonates (dolomite, aragonite and calcite), as well as Fe and Mn minerals (Supplementary Fig. 2). Diffraction peaks were matched to possible mineral phases using the tables in Chen (1977). Common Fe soil oxide minerals such as goethite and hematite could not be detected, but magnetite (d(Å) = 2.96, 1.60 and 1.53) and ankerite (d(Å) = 1.81), a Fe and Mn containing carbonate mineral closely related to dolomite, were both identified. Diffraction peaks diagnostic of pyrolusite (d(Å) = 3.15 Å), and periclase

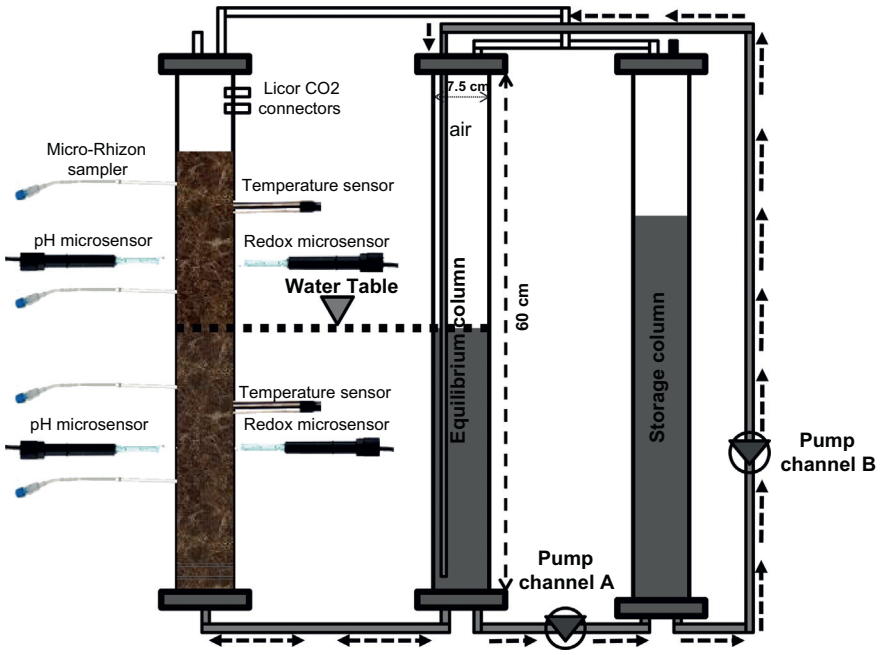

Fig. 1. Schematic diagram of the controlled water table column system.

(d(Å) = 1.49) support the presence of Mn oxides. Apatite (d(Å) = 2.21), a stable calcium phosphate mineral, was also detected.

2.3. Column instrumentation

The soil columns have 18 lateral ports (1/8″ NPT compression fittings) equally spaced every 3 cm. The ports are airtight and fitted with Teflon septa. For the experiment described here, four ports were equipped with ceramic samplers, 5 cm in length and 2.5 mm in diameter (CSS5 MicroRhizon™ samplers, Ejikelamp, Netherlands, #19.21.23F). The samplers were introduced horizontally into the soil matrix, at depths of −4, −12, −22 and −31 cm below the soil surface (Fig. 1). A vacuum pump (Soil Measurement Systems, LLC, USA, #CL-042) set at −100 mbar was used to extract pore water through the samplers. Aqueous samples for chemical analysis were collected weekly.

High-resolution redox potential (Eh) and pH microelectrodes (10 μM glass tip micro-electrodes, Unisense, Denmark) were installed at −10 and −30 cm depths through opposing ports (Fig. 1). Each pair of Eh and pH microelectrodes was combined with an external, micro-size reference electrode (open-ended Ag–AgCl electrode with gel-stabilized electrolyte, Unisense), which was in contact with the bottom outflow/inflow of the soil column. Electrode readings were recorded by a high-impedance (>10^{14} Ω) millivolt-meter (Unisense), which in turn was connected to the control computer. Platinum-wire electrodes and a high-resistance data logger were selected because they produce accurate and reliable Eh measurements (Rabenhorst et al., 2009). The Eh electrodes were calibrated with quinhydrone redox buffers (Sigma–Aldrich, #282960-25G), the pH electrodes with standard pH 4, 7, and 10 buffers (Thermo Orion). Two temperature sensors (DaqLink Fourier Systems Ltd., #DBSA720) occupied ports at −7 and −27 cm depth (see Fig. 1). The redox potential, pH and temperature were monitored every 60 s.

2.4. Water table regimes

The soil columns were packed under saturated conditions using creek water, and subsequently drained simultaneously until the water table reached a position 20 cm below the soil surface. In one of the columns, the water table was maintained at that position (−20 cm) from then on (stable water table column). In the other soil column, an oscillating water table regime was imposed (fluctuating water table column). To lower (raise) the water level, pump channel A (B) was activated (Fig. 1). The flow rate in both the upward and downward direction was 0.154 ml min^{-1}, which corresponds to a linear rate of 4.8 cm d^{-1}. The latter is typical of vertical rates of water table movement recorded in riparian areas of the Grand River watershed in recent decades (on average 4–5 cm d^{-1}; T. Patterson, Grand River Conservation Authority, pers. comm.). The water level oscillated between the soil surface (0 cm) and the bottom of the soil column (−45 cm), with an entire imbibition-drainage cycle lasting about 18–20 days. A water level data logger (Solinst, 3001 LT Levelogger Junior, M5/F15, #110241) continuously recorded the water level in the equilibrium column.

The experiment ran for 75 days at room temperature (25 ± 2 °C). Data were thus acquired on a time scale over which soil biogeochemistry and microbiology were expected to exhibit durable and distinctive changes in response to the imposed water table regimes. Special care was given to assessing the internal consistency of the time-series data. In the case of the fluctuating water table column, data acquisition over repeated cycles of water table rise and drawdown partly compensated for the absence of replicate experiments.

2.5. Analytical methods

2.5.1. Soil CO_2 flux

The headspace of the soil columns was sampled every 1–2 days by connecting it to an automated multiplexed CO_2 flux analyzer (Li-8100, Li-COR Biosciences, Lincoln, NE, USA) via two lateral ports (Fig. 1). During the measurements, the port allowing air to freely enter the column was closed. Air from the headspace above the soil was then circulated through the infrared gas analyzer (IRGA) of the Li-8100 and back to the column. The soil CO_2 flux F_{CO2} (μmol m^{-2} s^{-1}) was obtained from the rate at which the headspace CO_2 concentration increased ($dCco_2/dt$, μmol mol^{-1} s^{-1}) after closure from the outside atmosphere, according to

$$F_{co_2} = \frac{PV}{RTS}\frac{dC_{co_2}}{dt}$$

where P is the atmospheric pressure (Pa), V (m^3) is the volume of the headspace plus that of the sampling loop through which the headspace gas circulates, R is the gas constant (8.314 Pa m^3 K^{-1} mol^{-1}), T is the absolute temperature (K), and S (m^2) is the exposed soil surface area. The rate $dCco_2/dt$ was estimated from six consecutive 180 s observation windows spanning a 20 min time interval. Further details on the method can be found in Davidson et al., 2002; McDermitt et al., 2004; Norman et al., 1992).

2.5.2. Pore water geochemistry

To minimize the disturbance of the flow system, only small volumes (2 ml) of pore water were extracted through the MicroRhizon™ samplers (Cabrera, 1998; Knight et al., 1998). Integrated over the entire duration of the experiment, the weekly sampling from four depths amounted to approximately 5% of the total pore water in the soil columns. Immediately upon collection, the water samples were filtered through a 0.2 μm pore size polysulfone membrane filter and acidified with 2% HNO_3. Because of the small sample volumes, we opted to analyze total aqueous concentrations by Inductively Coupled Plasma Optical Emission Spectrometry (Thermo iCAP 6200 Duo ICP-OES) (McLaren et al., 1995). Concentrations of the following elements are reported: Fe, Mn, Si, K, Mg, Na, P and S.

2.5.3. Solid-phase geochemistry

At the end of the experiment, both soil columns were fully drained and disassembled. The soil was extruded via the top of the column using a lifting jack and sliced every 2 cm. The soil slices were homogenized and separate aliquots were taken for microbial and geochemical characterization. For the latter, samples were freeze-dried and stored at room temperature. Organic carbon concentrations (C_{org}) were measured on a CHNS Carbo Erba analyzer without any pre-treatment of the freeze-dried soil samples. Elemental compositions were determined after solubilization by microwave-assisted mineralization (Multiwave 3000, Anton-Parr) using 1 g soil in 12 ml aqua regia (9 ml 12 M HCl + 3 ml 16 M HNO_3). The extracts were recovered by centrifugation at 4500 rpm, followed by filtration on a 0.2 μm pore size polysulfone membrane (Link et al., 1998). Total concentrations of Fe, Mn, Si, K, Mg, Na, P and S in the extracts were measured by ICP-OES as described in the previous section. The same analyses were also performed on the original mixed soil used to fill the columns.

2.5.4. Geomicrobiology

The depth distributions of potential respiration rates in the soil columns at the end of the experiment were obtained directly on the sliced soil samples using the Micro-Resp™ method, which measures whole-soil CO_2 production under aerobic conditions (Artz et al., 2006; Campbell et al., 2003). The Micro-Resp™ system consists of a detection microplate, containing 150 μl purified agar (1%), cresol red indicator dye (12.5 μg ml^{-1}), potassium chloride (150 mM) and sodium bicarbonate (2.5 mM), and a 96-unit deepwell plate (1.2 ml wells). Triplicate 0.5 g soil samples were placed in the wells, covered with parafilm and incubated at 25 °C for 4 days. The detection plate was read with a spectrophotometer at absorbance wavelength 570 nm and then clamped to the deepwell plate using a rubber gasket and seal. The two-plate system was incubated for 6 h at 25 °C. The detection plate was then removed and read again with the spectrophotometer. The CO_2 production rates (respiration rates) were calculated from the differences between the absorbances measured at times 0 and 6 h (Campbell et al., 2003). A calibration curve for absorbance versus headspace equilibrium CO_2 concentration was determined by equilibrating dye solutions at different CO_2 concentrations prepared with standard gas mixtures and incubated for 6 h.

Total community DNA was extracted from soil samples (stored at −80 °C after slicing) with the PowerSoil DNA kit (MO BIO, Carlsbad, CA) following the manufacturer's instructions. The extracted DNA was visualized on 0.8% (w/v) agarose gel and DNA concentration and purity were assessed with a NanoDrop 2000c (Thermo Scientific). Polymerase chain reaction (PCR) was used to amplify 16S rRNA gene sequences. Bacterial 16S rRNA gene sequences were amplified with the universal primer pair 341F with GC clamp and 518R (Muyzer et al., 1993). The bacterial PCR thermal profile was: 95 °C for 5 min, 30 cycles at 95 °C for 1 min, 55 °C for 1 min, 72 °C for 1 min, and a final extension step at 72 °C for 7 min. Archaeal 16S rRNA gene sequences were amplified by nested PCR with the first primer pair 109F and 958R (DeLong, 1992; Jurgens et al., 1997); subsequently 1 μl of the first PCR product was used for a second PCR round with primer pair SA1F-GC & SA2F-GC and PARCH519R (Nicol et al., 2003; Ovreas et al., 1997). The Archaeal PCR thermal profile was: 95 °C for 5 min, then 35 cycles at 94 °C for 1 min, 45 °C for 1 min, 72 °C for 1 min, and a final extension step at 72 °C for 7 min. The second thermal profile was: 94 °C for 5 min, 35 cycles at 95 °C for 1 min, 53.5 °C for 1 min, 72 °C for 1 min, and a final extension at 72 °C for 7 min.

The PCR products were visualized by electrophoresis on 0.8% (w/v) agarose gels stained with ethidium bromide. The PCR products were used for Denaturing Gradient Gel Electrophoresis (DGGE) analysis. The DGGE gel contained 10% (w/v) polyacrylamide with a denaturing gradient of 30–70% (CBS Scientific Company). The gels ran for 14 h at 85 V (Green et al., 2010). The gels were stained with SYBR Green for an hour and visualized on a PharosFX Plus Molecular Imager (Bio-Rad, Hercules, CA). DGGE fingerprints were normalized and background subtraction was performed using GelCompar II (Applied Maths, Sint-Martens-Latem, Belgium). Cluster analysis was performed to construct similarity matrices based on the Pearson correlation coefficient and the Unweighted Pair Group Method using Arithmetic Averages (UPGMA) algorithm. Monte Carlo permutation testing was conducted to determine significance based on Sorensen (Bray-Curtis) distance matrices using PC-ORD (MJM Software Design, Gleneden Beach, OR). The Monte Carlo tests were based on 999 iterations, with a no relationship null hypothesis. Pearson correlation coefficients (r) were calculated to estimate correlation between community fingerprints.

3. Results and discussion

3.1. Water table and redox regimes

The experimental setup provides a precise control on the position of the water table in the soil columns for extended periods of time. The imposed water table regime, in turn, controls the spatial and temporal distributions of the soil oxidation–reduction potential (Eh) as illustrated in Figs. 2 and 3. In the stable water column, Eh values do not vary with time. The Eh values measured −10 and −30 cm below the soil surface are on the order of +600 and −200 mV, respectively. In the fluctuating water table soil column, the Eh measured at a given depth varies cyclically, in sink with the variations in water level. During drainage, conditions become more oxidizing, with Eh values increasing up to +700 mV, while during water table rise the Eh drops to negative values as low as −200 mV. (Sub)oxic conditions prevail about 75% of the time at a depth of −10 cm, but only 25% of the time at a depth of −30 cm. The time series Eh data recorded in the fluctuating water table soil column exhibit short-lived spikes. Similar Eh excursions have been observed in soils of tidal marshes and could reflect locally hetero-

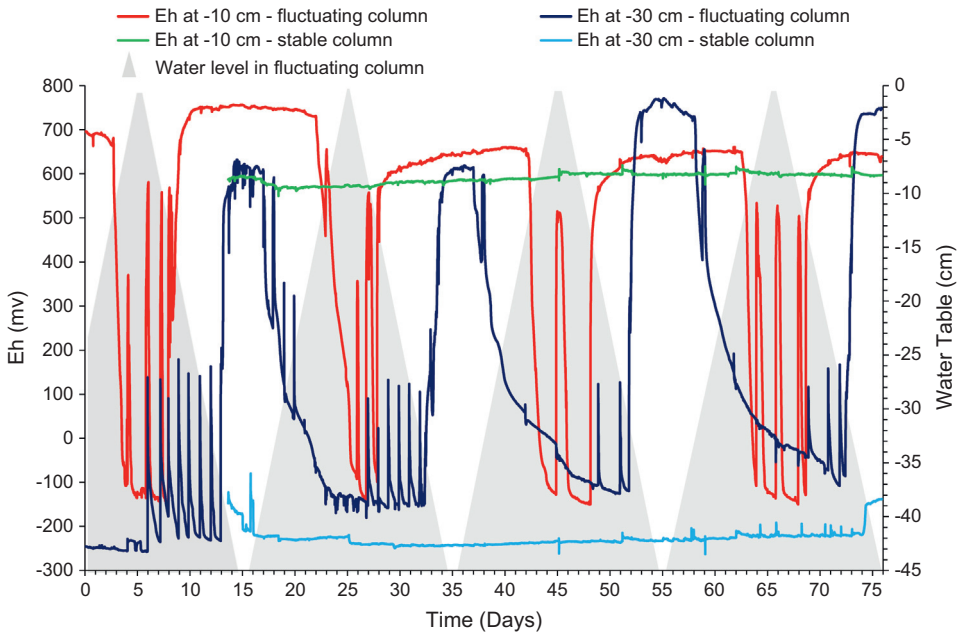

Fig. 2. Time series of the redox potential in the fluctuating and stable water table soil columns. Sampling points were located −10 and −30 cm below the soil surface in both columns.

geneous water and gas transport during water table fluctuations (Vorenhout et al., 2004).

A schematic representation of the time-dependent changes in the soil moisture (as a percentage of water-filled pores) and redox conditions at different depths in the fluctuating water table column is given in Fig. 4. In the upper portion of the soil column, that is, the topmost 15 cm, (sub)oxic and unsaturated conditions prevail most of the time. In the lower portion, that is, below −30 cm, anoxic and water saturated conditions are predominant. The upper and lower portions of the soil column are separated by a transition zone characterized by more evenly distributed periods of (sub)oxic/unsaturated and anoxic/saturated conditions. Our hypothesis is that with time the soil biogeochemistry and microbiology in the upper (lower) portion of the fluctuating column would become similar to those found above (below) the water table in the stable column, while they develop unique characteristics in the transition zone. This hypothesis is used as a framework for the analysis of the results discussed below.

3.2. Pore water geochemistry

Pore water pH values measured in the stable water table column are in the range 6–7, with slightly more alkaline conditions at a depth of −30 cm compared to −10 cm (Fig. 3). At both depths, pH varies within one unit over the course of the experiment. Pore water pH values in the fluctuating water table column cover a somewhat broader range than observed under stable water table conditions. In addition, they vary in concert with the water table fluctuations, with pH increasing slightly during water table rise and decreasing during drainage. Thermodynamic calculations show that, in both the stable and fluctuating water table columns, insoluble ferric iron oxyhydroxide mineral phases are stable under the redox and pH conditions encountered above the water table, while ferrous iron, in dissolved or mineral form, is stable under the Eh-pH conditions encountered below the water table (Fig. 3).

Aqueous iron (Fe) distributions are consistent with the thermodynamic predictions. In the pore water samples collected −4 and −12 cm below the soil surface, the concentrations of pore water Fe (presumably under the form of dissolved ferrous iron) are near or below detection in both soil columns (Fig. 5). In contrast, relatively high concentrations of aqueous Fe (on the order of 250 μM) are found below the water table in the stable column, as a result of the reductive dissolution of ferric iron mineral phases. In the fluctuating water table soil column, comparable high aqueous Fe concentrations are measured in the lower portion of the column (−31 cm). In the transition zone (−22 cm), however, aqueous Fe concentrations vary substantially depending on the position of the water table (Supplementary Figs. 3 and 4). The average pore water Fe concentration in the transition zone falls between those observed in the predominantly unsaturated (and (sub)oxic) upper and predominantly saturated (and anoxic) lower zones.

Elements whose pore water concentrations are closely tied to iron redox cycling exhibit depth and time series trends that parallel those of pore water Fe. This is particularly obvious for pore water phosphorus (Fig. 5 and Supplementary Figs. 3 and 4). As for aqueous Fe, total dissolved phosphorus (P) concentrations in the lower portion of the fluctuating water table column (−31 cm) are similar to those observed below the water table in the stable column (−22 and −31 cm). Pore water P concentrations in the transition zone of the fluctuating column, however, are significantly lower than observed at the same depth (−22 cm) in the stable water table column, because of the periodic recurrence of (sub)oxic conditions when the water table is lowered. The behavior of pore water P in the soil columns is consistent with the high sorption affinity of phosphate anions for ferric iron oxyhydroxides (Ruttenberg and Heinrich, 2003).

The observed distributions of pore water sulfur (S) concentrations can be explained along similar lines. The predominant form of pore water S is likely aqueous sulfate. Under the permanently reducing conditions encountered below the water table in the stable column (−22 and −31 cm), microbial sulfate respiration reduces sulfate to sulfide, which is subsequently removed from solution as sulfide mineral phases (Canfield et al., 2005). Near-zero pore water sulfate levels are also found at the deepest sampling point (−31 cm) in the fluctuating column, as highly reducing conditions prevail most of the time at this depth. In the transition zone of the fluctuating water table column (−22 cm), however, measurable pore water S concentrations persist, because of the periodic

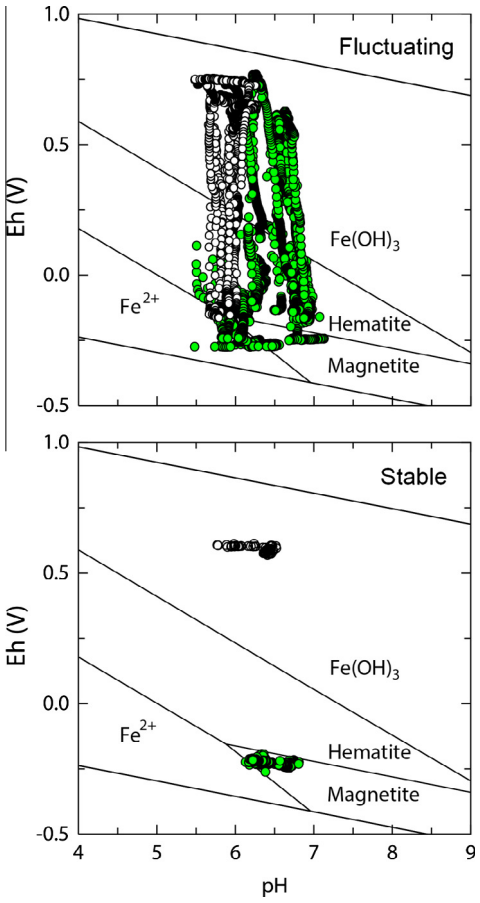

Fig. 3. Eh-pH diagrams for the Fe–O–H systems ($\Sigma Fe = 3 \times 10^{-4}$ M, 25 °C and 1 bar) and corresponding measurements in the the stable (upper panel) and fluctuating (lower panel) water table soil columns. In each panel, open and solid circles are Eh-pH couples for the sensors located in at −10 cm and −30 cm, respectively. Equilibrium calculations were performed with the public domain computer code PHREEQC Version 2.17.5 (Parkhurst and Apello, 1999) using the chemical composition of the pore waters. The diagrams were generated with the beta version of the public domain code PhreePlot (Kinniburgh and Cooper, 2009). The thermodynamic database WATEQ4F imbedded within PHREEQC was used.

recurrence of (sub)oxic conditions under which dissolved sulfate is stable.

In both soil columns, the pore water S concentrations are higher in the topmost samples (−4 cm), compared to those measured at a depth of −12 cm. While this may reflect more intense production of sulfate by sulfide oxidation under the more oxidizing conditions near the soil surface, evaporative concentration also contributes to the higher pore water S concentrations observed at −4 cm depth. The effects of purely physical processes on pore water concentrations can be inferred from the distributions of dissolved sodium (Na), which provides a conservative tracer not affected by changes in redox conditions. For instance, in the fluctuating water table column, pore water Na concentrations measured in the upper and lower portions diverge increasingly with time (Supplementary Fig. 4). Over the course of the experiment, the Na concentrations at −4 cm depth increase, due to evaporation, while they decrease at the three other sampling depths, due to admixing of more dilute water from the equilibrium column during the water level fluctuations.

In summary, the spatio-temporal distributions of redox-sensitive pore water constituents generally agree with the hypothesis that the biogeochemical differences between the stable and fluctuating water table columns are most pronounced in the mid-column depth interval. However, care must be taken to account for physical dilution and concentration effects when interpreting pore water concentrations in terms of biogeochemical processes.

3.3. Solid-phase geochemistry

The depth distributions of the extractable pools of a selected number of solid-phase elements collected at the end of the experiment are shown in Fig. 6. Particularly striking are the differences in the distributions of Fe, manganese (Mn), silicon (Si) and potassium (K) between the stable and fluctuating water table columns. Relative to the fluctuating column, the solid-phase concentrations of Fe, Mn, Si and K in the stable column are enriched in the upper 30 cm and depleted at greater depths. The depleted concentrations below −30 cm are lower than the initial concentrations of the homogenized soil (14.5, 0.3, 1.9 and 1.4 μmol g^{-1} for Fe, Mn, Si and K, respectively) and could therefore reflect dissolution of Fe, Mn, Si and K bearing mineral phases. For Fe and Mn, the main process is probably the reductive dissolution of Mn and Fe oxyhydroxide phases initially present in the riparian soil.

The concentrations of Fe and Mn in the upper 30 cm of the fluctuating column are below the initial soil concentrations. Most likely, Fe and Mn are solubilized by reductive dissolution during periods of water table rise and subsequently translocated to the lower portion of the soil column, or even partially removed to the equilibrium column, when the water is drained. This mechanism is consistent with the observed enrichments in solid-phase Fe and Mn below −35 cm (Fig. 6). A similar translocation mechanism also explains why the solid-phase concentrations of P and S in the lowermost 10 cm of the fluctuating water table soil column exceed the initial concentrations (1.1 and 0.9 μmol g^{-1} for P and S, respectively). The solid-phase S enrichment observed close to the soil surface (Fig. 6) may be caused by evaporative concentration of sulfate (see Section 3.2).

The results imply that the initially homogenous solid-phase distributions of reactive elements can be significantly modified on the time scale of the experiment. These modifications, however, differ markedly between the stable and fluctuating water table columns. In the latter, the observed redistributions of chemical elements reflect both the temporal variations in chemical conditions and the physical transport induced by the movement of the water table. Thus, in contrast to our original hypothesis, the solid-phase geochemical compositions of the upper and lower soil portions are diverging between the two columns, due to chemical transport associated with water rise and drawdown in the fluctuating water table column.

3.4. Soil microbiota

The PCR-DGGE fingerprinting shows no statistically significant differences ($p < 0.01$, $r = 0.94$) of the archaeal communities within or between the two soil columns (Fig. 7). This is consistent with the very slow rates at which Archaea tend to adapt to new environmental conditions (Konhauser, 2006). While somewhat larger differences are observed for the bacterial communities, the statistically most significant differences ($p > 0.10$, $r = -0.40$) are between the upper and lower portions in both soil columns. Thus, the bacterial communities inhabiting the (mostly) oxidizing and unsaturated upper portions of the soil columns and those in the lower, (mostly) reducing and saturated portions have begun to diverge on the time scale of the experiment (75 days). For the intermediate, transition zone, however, no systematic differences of the bacterial DGGE signatures are found between the two soil columns. This suggests that the noticeable differences in soil respiration (Section 3.5) and geochemistry under the fluctuating table regime, compared to the stable water table regime, primarily reflect

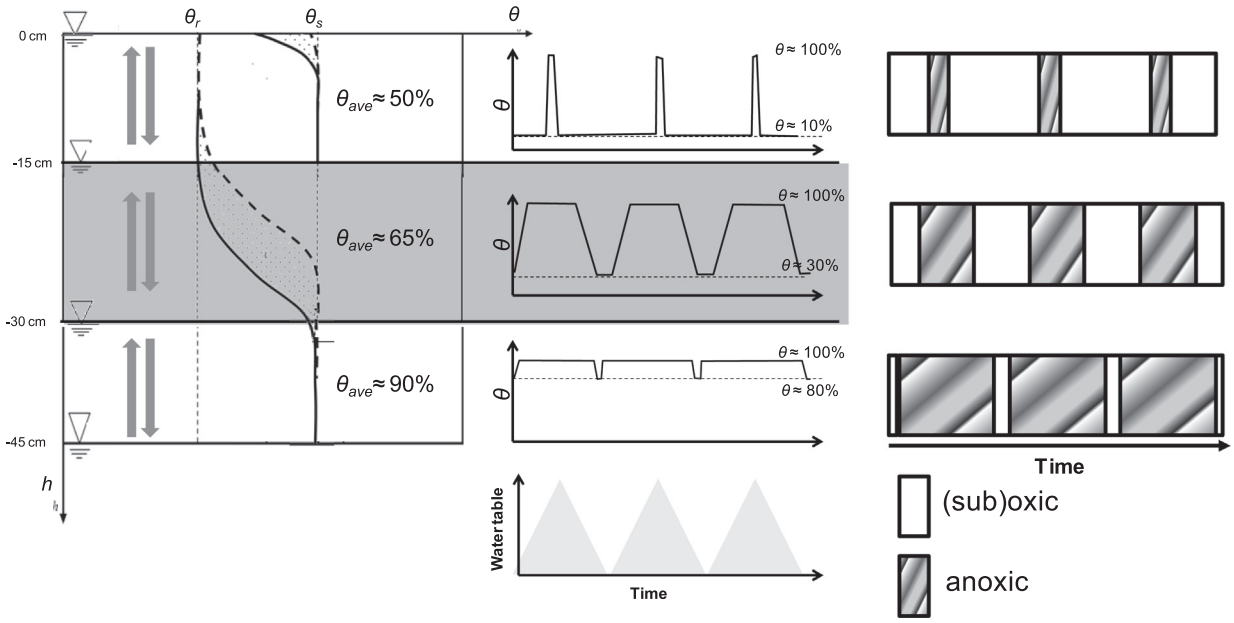

Fig. 4. Conceptual depth-time distributions of soil moisture (θ is defined as a percentage of water-filled pores) and redox conditions in the fluctuating water table column. The soil column is divided in an upper (0 to −15 cm), mostly (sub)oxic and unsaturated, zone, a lower (−30 to −45 cm), mostly anoxic and saturated, zone, and an intermediate transition zone (−15 to −30 cm). See text for further discussion.

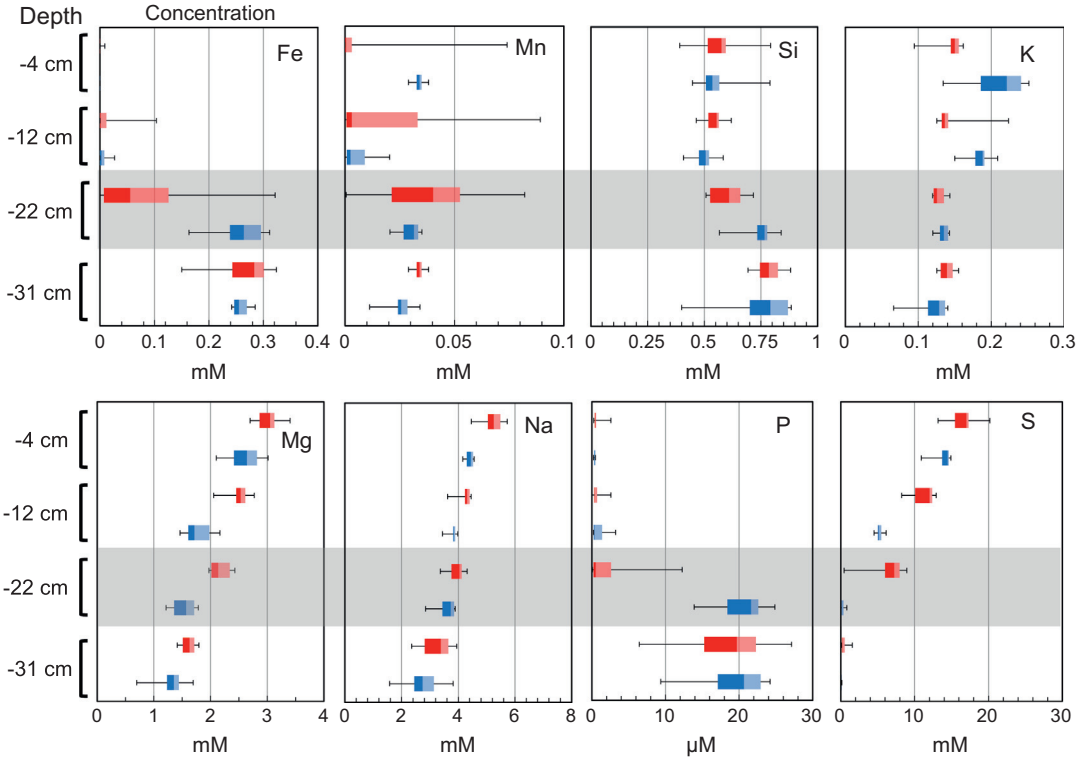

Fig. 5. Box plot representations of aqueous concentrations of Fe, Mn, Si, Na, Mg, K, P and S in the extracted pore water samples from different depths in the stable (blue boxes) and fluctuating (red boxes) water table soil columns. The gray shading indicates the transition zone. (For interpretation of the references to color in this figure legend, the reader is referred to the web version of this article.)

differences in activity of various components of the microbial community rather than major changes in community composition.

The bacterial community that at the end of the experiment is most closely related to the initial soil community is located near the base of the upper portion of the soil (−10 to −12 cm depth interval) in the fluctuating water table soil column. This depth interval also yields the strongest band intensities on the DGGE gel (Fig. 7). Thus, the original soil bacterial community appears to be well adapted to deal with the variable water saturation and redox conditions characterizing the fluctuating water table soil column. This is not unexpected given that the soil was collected from a riparian area that experiences water table fluctuations of similar

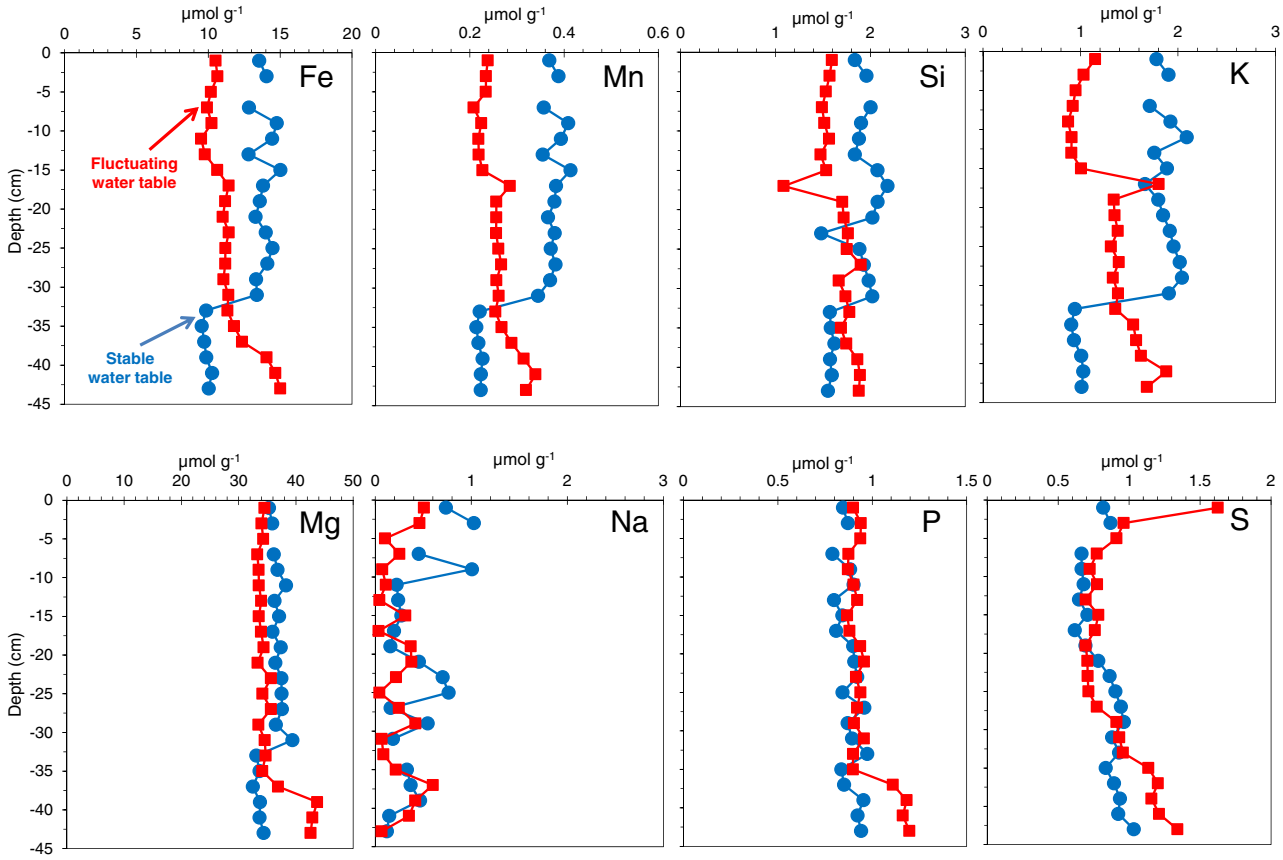

Fig. 6. Solid phase depth distribution of Fe, Mn, Si, Na, Mg, K, P and S in the fluctuating and stable water table soil columns at the end of the experiment.

magnitude and frequency as those imposed in the experiment (Section 2.4).

3.5. Soil respiration

The efflux of CO_2 from soils is a major component of the terrestrial carbon cycle (Raich and Schlesinger, 1992). Temperature and soil moisture are generally recognized as key environmental variables regulating the production of soil CO_2 (Davidson et al., 1998). In contrast, the effects on soil respiration of redox oscillations and water table fluctuations remain poorly known. One confounding factor when interpreting field-based CO_2 fluxes from intact soils is that autotrophic root respiration and heterotrophic microbial respiration may respond differently to variations in environmental conditions (Hanson et al., 2000). Because in the experiment described here live roots are absent, the following discussion focuses on the role of water table fluctuations in the turnover of organic carbon by soil microbiota and the associated efflux of CO_2.

The CO_2 efflux (F_{CO2}) from the stable water column falls within a fairly narrow range, 3.3–1.8 µmol m^{-2} s^{-1}, and exhibits a gentle decreasing trend with time (Fig. 8). These CO_2 fluxes fall within the range reported for temperate soils during summer months (e.g., Buchmann, 2000). In the fluctuating water table column, the much larger variations of F_{CO2} are clearly correlated with the water table fluctuations, with higher CO_2 fluxes coinciding with periods of water table drawdown. The highest F_{CO2} value (14.2 µmol m^{-2} s^{-1}) occurs during the first lowering of the water table, while subsequent F_{CO2} maxima rapidly decline in magnitude. Hence, despite the very high F_{CO2} values recorded in the fluctuating column during the initial stage of the experiment, the CO_2 effluxes from both columns tend to converge during the second half of the experiment.

Water table fluctuations affect F_{CO2} because of the accompanying changes in O_2 availability and water saturation. As the water table drops, O_2 penetrates deeper into the soil column, hence stimulating the mineralization of organic carbon to CO_2 by soil microorganisms (Chimner and Cooper, 2003; Lipson et al., 2012). Additionally, the upward movement of CO_2 is facilitated by smaller diffusion lengths and enhanced free gas transport as the unsaturated portion of the soil expands during water drawdown. In both columns, the decreasing trends of F_{CO2} with time can be explained by a decreasing availability of labile organic substrates. Because respiration is initially higher in the fluctuating column, the pool of labile soil organic matter is depleted faster than in the stable column, hence causing a more rapid attenuation of respiratory activity. As discussed below, this explanation is consistent with the potential CO_2 production rates and the particulate organic carbon depth distributions measured at the end of the experiment (Fig. 9).

As shown in Fig. 9, below −15 cm depth the potential CO_2 production rates measured in the Micro-Resp™ assays on the soil samples collected at the end of the experiment are systematically lower in the fluctuating water table column. The rates further show a distinct minimum in the transition zone (−15 to −30 cm). The transition zone also exhibits a minimum in particulate organic carbon concentration. Neither the potential CO_2 production rates nor the particulate organic carbon concentrations show a similar feature in the stable water table column. These observations are attributed to a more efficient mineralization of organic matter under the conditions encountered in the transition zone of the fluctuating water table column. As a result, at the end of the experiment this zone is depleted in labile organic matter, hence limiting the potential respiratory rates.

Although pore water DOC concentrations were not measured, a simple back-of-the-envelope calculation shows that preferential

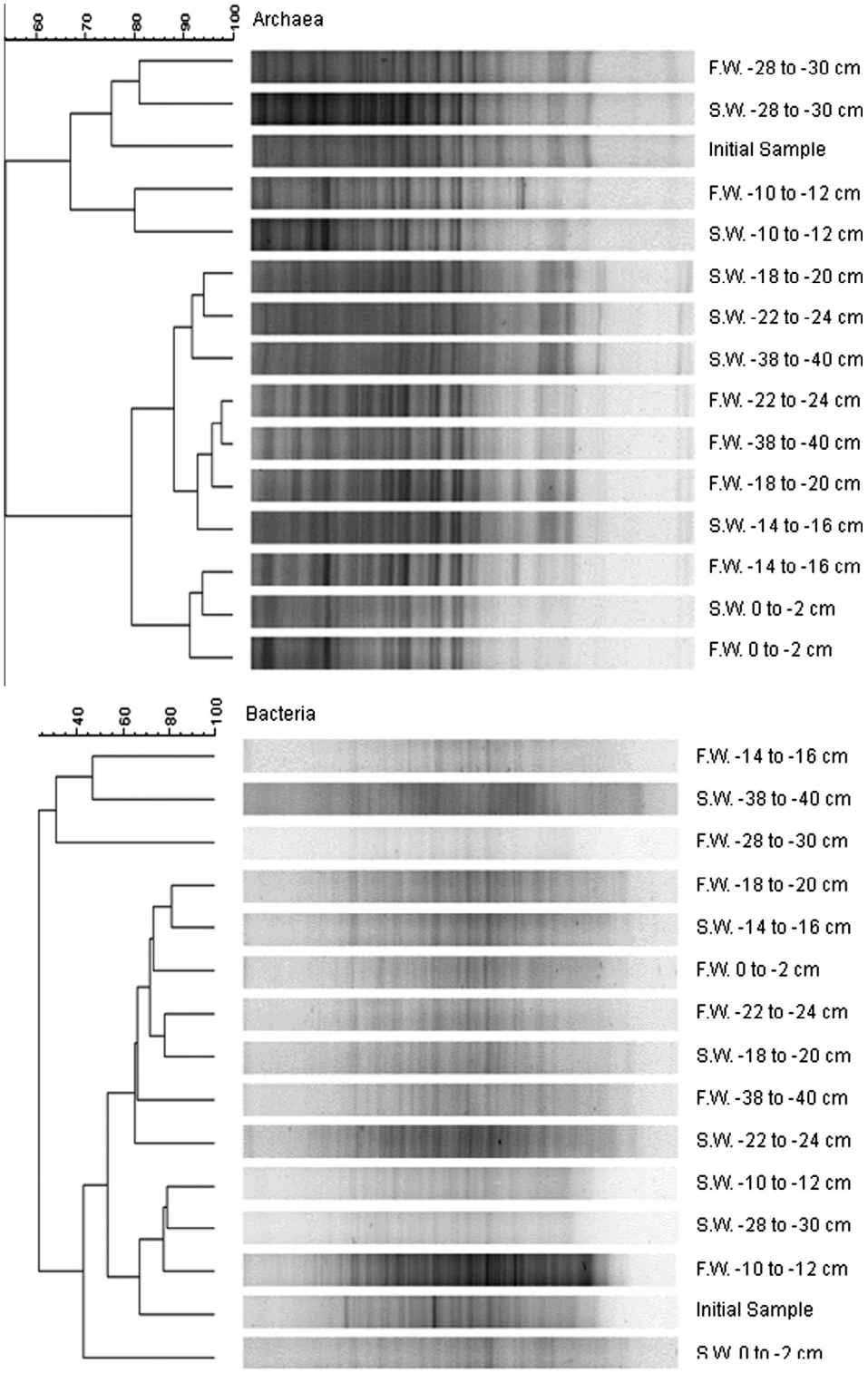

Fig. 7. Dendrograms for Archaeal and Bacterial 16S rRNA gene fingerprints created using the PCR-DGGE method on soil samples collected at the end of the experiment. FW and SW indicate the fluctuating and stable water table columns, respectively.

leaching and export of DOC cannot explain the observed loss of particulate carbon from the transition zone in the fluctuating water table column (Fig. 9). Using the cumulative volume of water removed from the soil column during the successive drainage periods (3.5 l) and assuming an upper limit of 50 mg l^{-1} for the DOC concentration, the removal of DOC amounts to about 175 mg C. In comparison, the loss of particulate carbon from the transition zone is on the order of 2000 mg, assuming a bulk density of 1.04 g cm^{-3}. Thus, DOC export could at most account for 9% of the particulate carbon loss from the mid-section of the fluctuating water table column. Note that this is an absolute maximum estimate, as DOC concentrations on the order of 50 mg l^{-1} are only observed in organic peat soils under low-runoff conditions (Thurman, 1985). In addition, such high DOC concentrations would impart a

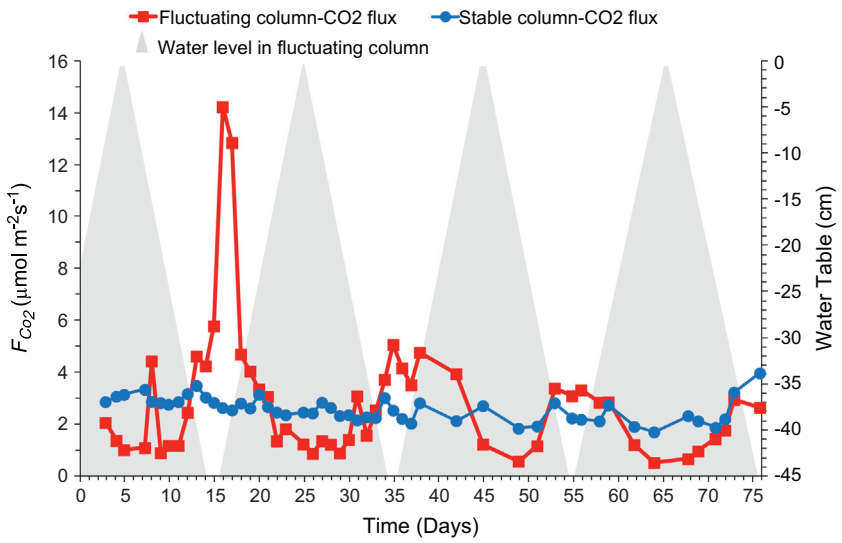

Fig. 8. Efflux of CO_2 in the fluctuating and stable water table columns plotted as a function of time. The plot also shows the water table depth in the fluctuating column.

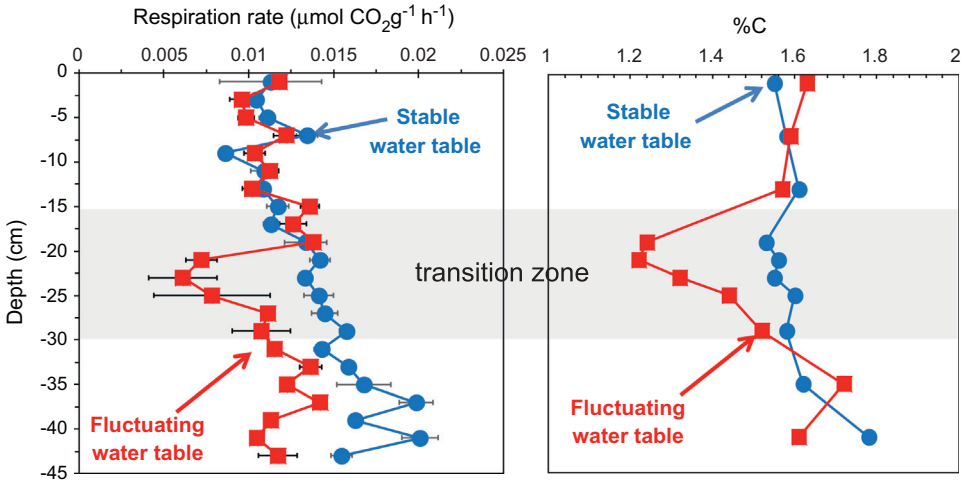

Fig. 9. Vertical distributions of potential CO_2 production rates (left) and concentrations of particulate organic carbon (right) in the fCHNSC.

distinctive dark color to the water, which was not observed during the experiment.

Several studies have shown that fluctuating redox conditions arising from alternate wetting and drying enhance soil organic carbon turnover (Fierer and Schimel, 2002; Smith and Patrick, 1983; Odum, 1983; Pett-Ridge and Firestone, 2005). Redox oscillations have also been proposed to result in a more complete degradation of organic matter in bioturbated marine sediments (Aller, 1994). Thus, we propose that fluctuating redox conditions are in part responsible for the minima in organic carbon concentration and potential CO_2 production rates in the transition zone of the fluctuating column observed at the end of the experiment. Variations in soil moisture content likely impose additional constraints, however (Franzluebbers, 1999; Konopka and Turco, 1991; Linn and Doran, 1984).

Results from a variety of studies, involving a wide range of soils, show that soil moisture contents on the order of 60% tend to maximize soil respiratory activity (Table 1 in Linn and Doran, 1984). The Micro-Resp™ assays performed at different soil moisture contents under aerobic conditions confirm that CO_2 production rates are highest for moisture contents near 60% (Supplementary Fig. 5). Thus, the enhanced organic matter decomposition in the transition zone of the fluctuating water table column can be attributed to the combination of fluctuating redox conditions and optimal water content, while the drier and wetter conditions prevailing in the upper and lower sections of the soil column, respectively, limit CO_2 production.

4. Summary and conclusions

In this paper, we introduce a soil column system in which the position of the water table is controlled by a programmable pump. The system allows the user to impose any predefined water table regime of his/her choice. It is therefore particularly well suited for studies designed to advance the mechanistic understanding of the interactions between water table dynamics and biogeochemical processes and fluxes in the transition zone separating the soil from the underlying groundwater reservoir. To illustrate the potential applications of the soil column system, we present the results of a comparative study with two parallel columns filled with the same homogenized riparian soil. The water table is kept at a constant level in one column, while in the other the water table oscillates between the top and bottom of the soil column.

Differences in the pore water distributions of redox-sensitive elements (Fe, Mn, P, S) are most pronounced in the mid-section portions of the columns where the contrast in redox conditions between the two columns is largest. Differences in solid-phase geochemistry observed at the end of the experiments (11 weeks) show that, in addition to variable redox conditions, advective transport also contributes to the redistribution of chemical elements in the fluctuating column. In particular, mobilization during water table rise and subsequent downward transport during drainage explains the enrichments of solid-phase Fe, Mn, P, S and Mg observed in the lowermost section of the fluctuating water table column.

The comparative analysis of the microbial communities in the columns at the end of the experiment reveals little differences for the Archaea, while some differences in bacterial DNA emerge between the upper (oxidizing) and lower (reducing) soil portions in both columns. Although no systematic differences in microbial community structure could be found between the two columns, the CO_2 emissions were clearly affected by the imposed water table regimes. The water table variations led to a faster depletion of soil organic matter in the mid-section region of the fluctuating water table column. The results indicate that the oscillating redox conditions in this depth interval, together with a water saturation level on the order of 60%, stimulates microbial respiratory activity and, hence, soil organic carbon turnover.

Currently, there is great interest in understanding the response of soil respiration to environmental drivers as it represents a major source of carbon to the atmosphere. Existing models of soil respiration emphasize the importance of soil moisture, temperature and primary productivity as regulating environmental factors (Xu et al., 2004). The results of this study identify redox oscillations as an additional control on soil carbon turnover and, consequently, CO_2 emissions to the atmosphere. As a corollary, any changes in the redox dynamics of a soil, caused for example by changes in weather patterns, flooding frequency, or irrigation and drainage practices, have the potential to modify the production and efflux of CO_2. More research is required, however, to fully unravel the mechanisms linking oscillating redox conditions to soil microbial activity, and disentangle the relative effects of variations in redox conditions, water content and water table movement.

Acknowledgements

Special thanks go to Pieter Kleingeld for his generous help during the construction of the column system. We thank Dr. Kristin Mueller, Marianne Vander Griendt, Yris Verastegui and Margarita Rashev for their assistance with sample analysis. We are indebted to Dr. Josh D. Neufeld for providing the facilities for microbial analysis and for helpful discussions during data analysis. Funding was provided by the Canada Excellence Research Chair (CERC) program.

Appendix A. Supplementary material

Supplementary data associated with this article can be found, in the online version, at http://dx.doi.org/10.1016/j.jhydrol.2013.11.036.

References

Aller, R.C., 1994. Bioturbation and remineralization of sedimentary organic matter: effects of redox oscillation. Chem. Geol. 114, 331–345.
Artz, R.R.E., Chapman, S.J., Campbell, C.D., 2006. Substrate utilization profiles of microbial communities in peat are depth dependent and correlate with whole soil FTIR profiles. Soil Biol. Biochem. 38, 2958–2962.
Blodau, C., Moore, T.R., 2003. Micro-scale CO_2 and CH_4 dynamics in a peat soil during a water fluctuation and sulfate pulse. Soil Biol. Biochem. 35, 535–547.
Borch, T., Kretzschmar, R., Kappler, A., Van Cappellen, P., Ginder-Vogel, M., Voegelin, A., Campbell, K., 2010. Biogeochemical redox processes and their impact on contaminant dynamics. Environ. Sci. Technol. 44, 15–23.
Bubier, J., Moore, T.R., Juggins, S., 1995. Predicting methane emission from bryophyte distribution in northern peatlands. Ecology 76, 677–693.
Buchmann, N., 2000. Biotic and abiotic factors controlling soil respiration rates in Picea abies stands. Soil Biol. Biochem. 32, 1625–1635.
Cabrera, R.I., 1998. Monitoring chemical properties of container growing media with small soil solution samplers. Sci. Hortic. 75, 113–119.
Campbell, C.D., Chapman, S.J., Cameron, C.M., Davidson, M.S., Potts, J.M., 2003. A rapid microtiter plate method to measure carbon dioxide evolved from carbon amendments so as to determine the physiological profiles of soil microbial communities by using whole soil. Appl. Environ. Microbiol. 69, 3593–3599.
Canfield, D., Kristensen, E., Thamdrop, B., 2005. Thermodynamics and Microbial Metabolism. In: Southward, A.J., Tyler, P.A., Young, C.M., Fuiman, L.A. (Eds.), Aquatic Geomicrobiology, 48, 2005.
Chen, P.Y., 1977. Table of Key Lines in X-ray Powder Diffraction Patterns of Minerals in Clays and Associated Rocks. Department of Natural Resources, Geol. Surv. Occasional Paper, 21. Bloomington, Indiana.
Chimner, R.A., Cooper, D.J., 2003. Influence of water table levels on CO_2 emissions in a Colorado subalpine fen: an in situ microcosm study. Soil Biol. Biochem. 35, 345–351.
Davidson, E.A., Belk, E., Boone, R.D., 1998. Soil water content and temperature as independent or confounded factors controlling soil respiration in a temperate mixed hardwood forest. Glob. Change Biol. 4, 217–222.
Davidson, E.A., Savage, K., Verchot, L.V., Navarro, R., 2002. Minimizing artifacts and biases in chamber-basedmeasurements of soil respiration. Agric. For. Meteorol. 113, 21–37.
DeLong, E.F., 1992. Archaea in coastal marine environments. Proc. Natl. Acad. Sci. USA 89, 5685–5689.
Dobson, R., Schroth, M.H., Zeyer, J., 2007. Effect of water-table fluctuation on dissolution and biodegradation of a multi-component, light nonaqueous-phase liquid. J. Contam. Hydrol. 94, 235–248.
Drenovsky, R.E., Vo, D., Graham, K.J., Scow, K.M., 2004. Soil water content and organic carbon availability are major determinants of soil microbial community composition. Microb. Ecol. 48, 424–430.
Farnsworth, C.E., Voegelin, A., Hering, J.G., 2012. Manganese oxidation induced by water table fluctuations in a sand column. Environ. Sci. Technol. 46, 277–284.
Fierer, N., Schimel, J.P., 2002. Effects of drying-rewetting frequency on soil carbon and nitrogen transformations. Soil Biol. Biochem. 34, 777–787.
Franzluebbers, A.J., 1999. Microbial activity in response to water-filled pore space of variably eroded southern Piedmont soils. Appl. Soil Ecol. 11, 91–101.
Gardner, W.H., 1986. Water content. In: Kiute, A. (Ed.), Methods of Soil Analysis: Physical and Mineralogical Methods, Agronomy Series 9 (Part 1). Soil Science Society of America, Madison, Wisconsin, pp. 493–544.
Green, S.J., Leigh, M.B., Neufeld, J.D., 2010. Denaturing gradient gel electrophoresis (DGGE) for microbial community analysis. In: Timmis, K. (Ed.), Hydrocarbon Microbiology. Springer, Berlin, Heidelberg, pp. 4137–4158.
Griffiths, B.S., Hallett, P.D., Kuan, H.L., Pitkin, Y., Aitken, M.N., 2005. Biological and physical resilience of soil amended with heavy metal-contaminated sewage sludge. Eur. J. Soil Sci. 56, 197–206.
Haberer, C.M., Rolle, M., Cirpka, O.A., Grathwohl, P., 2012. Oxygen transfer in a fluctuating capillary fringe. Vadose Zone J. 11 (3). http://dx.doi.org/10.2136/vzj2011.0056.
Hancock, P.J., Boulton, A.J., Humphreys, W.F., 2005. Aquifers and hyporheic zones: towards an ecological understanding of groundwater. Hydrogeol. J. 13, 98–111.
Hanson, P.J., Edwards, N.T., Garten, C.T., Andrews, J.A., 2000. Separating root and soil microbial contribution to soil respiration. A review of methods and observations. Biogeochemistry 48, 115–146.
Hefting, M., Clément, J.C., Dowrick, D., Cosandey, A.C., Bernal, S., Cimpian, C., Tatur, A., Burt, T.P., Pinay, G., 2004. Water table elevation controls on soil nitrogen cycling in riparian wetlands along a European climatic gradient. Biogeochemistry 67, 113–134.
Jurgens, G., Lindstrom, K., Saano, A., 1997. Novel group within the kingdom crenarchaeota from boreal forest soil. Appl. Environ. Microbiol. 63, 803–805.
Kinniburgh, D.G., Cooper, D.M., 2009. PhreePlot-Creating graphical output with PHREEQC.
Klute, A., Dirksen, C., 1986. Hydraulic conductivity and diffusivity: laboratory methods. In: Klute, A. (Ed.), Methods of Soil Analysis. Soil Science Society of America, Madison, WI, pp. 687–734.
Knight, B.P., Chaudri, A.M., McGrath, S.P., Giller, K.E., 1998. Determination of chemical availability of cadmium and zinc in soils using inert soil moisture samplers. Environ. Pollut. 99, 293–298.
Konhauser, K., 2006. Introduction to Geomicrobiology. Blackwell Publishing, Malden, 440 pp.
Konopka, A., Turco, R., 1991. Biodegradation of organic compounds in vadose zone and aquifer sediments. Appl. Environ. Microbiol. 57, 2260–2268.
Legout, C., Molenat, J., Hamon, Y., 2009. Experimental and modeling investigation of unsaturated solute transport with water-table fluctuation. Vadose Zone J. 8, 21–31.
Link, D.D., Walter, P.J., Kingston, H.M., 1998. Development and Validation of the New EPA Microwave-Assisted Leach Method 3051A. Environ. Sci. Technol. 32, 3628–3632.
Linn, D.M., Doran, J.W., 1984. Effect of water-filled pore space on carbon dioxide and nitrous oxide production in tilled and nontilled soils. Soil Sci. Soc. Am. J. 48, 1267–1272.

Lipson, D.A., Zona, D., Raab, T.K., Bozzolo, F., Mauritz, M., Oechel, W.C., 2012. Water-table height and microtopography control biogeochemical cycling in an Arctic coastal tundra ecosystem. Biogeosciences 9, 577–591.

McDermitt, D.K., Welles, J.M., Madsen, R.A., Garcia, R.L., 2004. Analysis of soil CO_2 efflux data. Theoretical considerations and comparison of two measurement approaches. Oral Presentation at Annual Meeting of ASA-CSSA-SSSA. Seattle, WA. October 31–November 3, 2004.

McLaren, J.W., Methven, B.A.J., Lam, J.W.H., Berman, S.S., 1995. The use of inductively coupled plasma mass spectrometry in the production of environmental certified reference materials. Mikrochim. Acta 119, 287–295.

Moore, T.R., Knowles, R., 1989. The influence of water table levels on methane and carbon dioxide emissions from peatland soils. Can. J. Soil Sci. 69, 33–38.

Muyzer, G., de Waal, E.C., Uitterlinden, A.G., 1993. Profiling of complex microbial populations by denaturing gradient gel electrophoresis analysis of polymerase chain reaction-amplified genes coding for 16S rRNA. Appl. Environ. Microbiol. 59, 695–700.

Nicol, G.W., Glover, L.A., Prosser, J.I., 2003. The impact of grassland management on archaeal community structure in upland pasture rhizosphere soil. Appl. Environ. Microbiol. 5, 152–162.

Norman, J.M., Garcia, R., Verma, S.B., 1992. Soil surface CO_2 fluxes and the carbon budget of a grassland. J. Geophys. Res. 97, 845–853.

Odum, E.P., 1983. Basic Ecology. Sanders College Publishing, Philadelphia, Penn.

Ovreas, L., Forney, L., Daae, F.L., Torsvik, V., 1997. Distribution of bacterioplankton in meromictic Lake Saelenvannet, as determined by denaturing gradient gel electrophoresis of PCR-amplified gene fragments coding for 16S rRNA. Appl. Environ. Microbiol. 63, 3367–3373.

Parkhurst, D.L., Apello, C.A.J., 1999. User's Guide to PHREEQC (Version 2), a computer program for speciation, batch reaction, one-dimensional transport, and inverse geochemical calculations. In Water-Resources Investigations Report 99–4259, Denver, Colorado, p. 312 +xiv.

Pett-Ridge, J., Firestone, M.K., 2005. Redox fluctuation structures microbial communities in a wet tropical soil. Appl. Environ. Microbiol. 71, 6998–7007.

Pett-Ridge, J., Silver, W.L., Firestone, M.K., 2006. Redox fluctuations frame microbial community impacts on N-cycling rates in a humid tropical forest soil. Biogeochemistry 81, 95–110.

Pulleman, M., Tietema, A., 1999. Microbial C and N transformations during drying and rewetting of coniferous forest floor material. Soil Biol. Biochem. 31, 275–285.

Rabenhorst, M.C., Hively, W.D., James, B.R., 2009. Measurements of soil redox potential. Soil Sci. Soc. Am. J. 73, 668–674.

Raich, J.W., Schlesinger, W.H., 1992. The global carbon dioxide flux in soil respiration and its relationship to vegetation and climate. Tellus 44B, 81–99.

Ruttenberg, K.C., Heinrich, D.H., 2003. The Global Phosphorus Cycle. Treatise on Geochemistry, Oxford, Pergamon, pp. 585–643.

Schimel, J., Balser, T.C., Wallenstein, M., 2007. Microbial stresses response physiology and its implications for ecosystem function. Ecology 88, 1368–1394.

Sinke, A.J.C., Dury, O., Zobrist, J., 1998. Effects of a fluctuating water table: column study on redox dynamics and fate of some organic pollutants. J. Contam. Hydrol. 33, 231–246.

Smith, C.J., Patrick, W.H., 1983. Nitrous oxide emission as affected by alternate anaerobic and aerobic conditions from soil suspensions enriched with ammonium sulphate. Soil Biol. Biochem. 15, 693–697.

Sophocleous, M., 2002. Interactions between groundwater and surface water: the state of the science. Hydrogeol. J. 10, 52–67.

Thurman, E.M., 1985. Organic geochemistry of natural waters. Kluwer, Dordrecht, pp. 497.

Triska, F.J., Kennedy, V.C., Avanzino, R.J., Zellweger, G.W., Bencala, K.E., 1989. Retention and transport of nutrients in a third-order stream in northwestern California: hyporheic processes. Ecology 70, 1893–1905.

Trolard, F., Bourrie, G., Abdelmoula, M., Refait, P., Feder, F., 2007. Fougerite, a new mineral of the pyroaurite – iowaite group: description and crystal structure. Clays Clay Miner. 55, 323–334.

Vorenhout, M., van der Geest, H.G., van Marum, D., Wattel, K., Eijsackers, H.J.P., 2004. Automated and continuous redox potential measurements in soil. J. Environ. Qual. 33, 1562–1567.

Weber, F.-A., Voegelin, A., Kaegi, R., Kretzschmar, R., 2009. Biogenic copper(0) and metal sulphide colloids mobilize contaminants in flooded soil. Nat. Geosci. 2, 267–271.

Williams, M.D., Oostrom, M., 2000. Oxygenation of anoxic water in a fluctuating water table system: an experimental and numerical study. J. Hydrol. 230, 70–85.

Xu, L., Baldocchi, D.D., Tang, J., 2004. How soil moisture, rain pulses, and growth alter the response of ecosystem respiration to temperature. Global Biogeochem. Cycles 18. http://dx.doi.org/10.1029/2004GB002281.

Yavitt, J.B., Williams, C.J., Wieder, R.K., 1997. Production of methane and carbon dioxide in peatland ecosystems across North America: effects of temperature, aeration, and organic chemistry of the peat. Geomicrobiol J. 14, 299–316.